immuno

MDPI

Article

Characterization of Extracellular Vesicle-Enriched Populations in B-Cell Acute Lymphoblastic Leukemia from Peripheral Blood

Miguel Angel Carmona-Zamudio [1,2], Francisco Sierra-López [1], Carlos Emilio Miguel-Rodríguez [1], Maricarmen Hernández-Rodríguez [2], Gustavo Acosta-Altamirano [3] and Mónica Sierra-Martínez [1,*]

[1] Unidad de Investigación en Salud, Hospital Regional de Alta Especialidad de Ixtapaluca, Servicios de Salud de Instituto Mexicano del Seguro Social para el Bienestar (IMSS-Bienestar), Carr. Mex-Puebla Km 34.5 Col., Zoquiapan, Mexico City 56530, Mexico; carmona.zamudio.hraei@gmail.com (M.A.C.-Z.); carlos_emilio_13@hotmail.com (C.E.M.-R.)

[2] Laboratorio de Cultivo Celular, Sección de Posgrado e Investigación, Escuela Superior de Medicina, Instituto Politécnico Nacional, Plan de San Luis y Salvador Diaz Mirón S/N, Mexico City 11340, Mexico; dra.hernandez.ipn@gmail.com

[3] Hospital General de Mexico "Dr. Eduardo Liceaga", Eje 2A Sur (Dr. Balmis) No. 148, Cuauhtémoc, Doctores, Mexico City 06726, Mexico; gustavo.acostaa@salud.gob.mx

* Correspondence: msierra.hraei@imssbienestar.gob.mx; Tel.: +52-555-972-9800

Abstract

Extracellular vesicles (EVs) are lipid bilayer-bound structures capable of transporting molecular markers from their cell of origin and are secreted by multiple cell types, including malignant cells. EVs have emerged as promising tools for developing less invasive diagnostic approaches. In B-cell acute lymphoblastic leukemia (B-ALL), immunophenotypic characterization of extracellular vesicle-enriched populations (EVEPs) in peripheral blood (PB) may provide complementary information for disease detection and monitoring. This exploratory study aimed to characterize EVEPs obtained from PB and bone marrow (BM) of adult patients with B-ALL and to compare them with the clinical immunophenotype (CIP). A total of 12 individuals were initially recruited (eight with B-ALL, one with T-ALL, and three healthy controls). The study focused on the eight B-ALL patients and three controls, while the T-ALL sample was used as a specificity control. EVEPs were isolated by differential centrifugation and analyzed by flow cytometry and confocal microscopy, primarily evaluating CD3 and CD19 expression. EVEPs derived from PB samples of patients with B-ALL showed a higher percentage of marker-positive events by flow cytometry (CD45, CD34, CD19, CD20, and CD10), consistent with the leukemic phenotype identified in the CIP. Additionally, $CD3^+CD19^+$ EVEPs were occasionally detected. These findings suggest that EVEPs partially reflect the leukemic immunophenotype and may serve as a complementary source of biological information. The detection of $CD3^+CD19^+$ events highlights complex cellular interactions within the leukemic niche and warrants further investigation.

Keywords: extracellular vesicles (EVs); $CD3^+$ $CD19^+$; B-cell acute lymphoblastic leukemia

Check for updates

Academic Editors: Pierpaolo Di Micco and Ming-Lin Liu

Received: 2 March 2026
Revised: 9 April 2026
Accepted: 30 April 2026
Published: 6 May 2026

Copyright: © 2026 by the authors. Licensee MDPI, Basel, Switzerland. This article is an open access article distributed under the terms and conditions of the Creative Commons Attribution (CC BY) license.

1. Introduction

Extracellular vesicles (EVs) are nanometric structures delimited by a lipid bilayer that play a crucial role in intercellular communication by transporting biomolecules such as proteins, nucleic acids, and lipids [1–3]. EVs include subpopulations such as exosomes (30–150 nm) and microvesicles (100 nm–1 μm) [4–6].

In the context of oncology, it has been observed that various neoplastic cells can release abundant amounts of EVs, which have been associated with tumor progression,

immunomodulation, and the formation of metastatic niches [7–9]. In the specific case of leukemia, elevated levels of EVs have been documented in peripheral blood (PB), which have been associated with participating in leukemic transformation, promoting cell survival, and altering the bone marrow (BM) microenvironment [10–12], as has been suggested in other types of cancer [6,7,13–18].

While the diagnosis of acute lymphoblastic leukemia (ALL) is currently based on invasive methods such as BM aspiration, followed by flow cytometry, cytogenetics, and molecular biology techniques [19–25], translational research has explored the potential of EVs as a source of less invasive biomarkers in PB [3,26–28]. Traditional experiments with EVs have focused on the evaluation of small EVs (mainly exosomes) and, secondarily, large EVs (mainly microvesicles) [29,30]. Although methodologies exist that seek to purify extracellular vesicles, biological processes still interfere with selectivity, so absolute purity cannot be achieved in the isolation of EV populations [31,32]; their joint study could provide a greater number of markers of interest, including cell surface markers, in addition to showing intervesicular fusion phenomena that could occur in vivo [33–36]. It might also provide evidence suggesting the presence or absence of abnormal cells, even when these are at levels undetectable by routine strategies.

There are currently several methods for characterizing EVs; one of these involves surface proteins, also known as CDs, which have played a crucial role in this characterization, primarily through the use of flow cytometry. This has enabled the identification of tetraspanins such as CD9, CD63 and CD81, which are widely recognized as canonical markers of EVs [8,37,38]. Furthermore, lineage-specific markers, such as CD19 and CD10 for B cells and CD3 for T cells, are essential for immunophenotypic characterization [39].

Markers such as CD34 and CD20 further contribute to the identification of cellular differentiation and maturation states. Therefore, the selection of these markers allows not only for the identification of EVs, but also for the exploration of their potential cellular origin and biological relevance in leukemic contexts [40,41].

The cargo that can be contained in EVs secreted by B-ALL or T-ALL cells includes markers specific to leukemia, which has suggested the use of these EVs for the diagnosis and monitoring of the disease. B-ALL EVs can carry markers such as CD19, CD20, and CD10 [42,43], while T-ALL EVs can carry markers such as CD3 [44,45].

The existence of a rare lymphocyte subpopulation has recently been described. This population is characterized by the co-expression of T-lineage (CD3) and B-lineage (CD19) markers and represents approximately 0.16% of total lymphocytes in healthy donors, which was significantly more highly expressed in patients with various solid neoplasms (approximately 0.58%) [34], a cell subpopulation that has also been identified in murine models [42,43]. It has been established that EVs contain membrane proteins from their cell of origin [44,45], suggesting two non-mutually exclusive mechanisms for the generation of double-positive $CD3^+CD19^+$ EVs: (1) direct secretion by leukemic lymphoblasts exhibiting an aberrant dual immunophenotype, a well-characterized phenomenon in leukemia of ambiguous lineage [46] and reported in solid cancers as well as in healthy murine and human models [34,43], or (2) post-secretion fusions between $CD19^+$ microvesicles derived from B lymphoblasts and $CD3^+$ microvesicles derived from T lymphocytes, a mechanism facilitated by the high vesicular concentration and favorable conditions of the leukemic microenvironment [15,32,35,47].

The detection of these EVs could in itself offer a molecular reflection of cellular dynamics that could be considered aberrant, as has been observed with some other oncogenic receptors [48], providing a unique window to investigate biological processes underlying ALL through liquid biopsy [13,29,49].

Considering the current recommendations in 'Minimal information for studies of extracellular vesicles' (MISEV) 2018 and 2023 [30,33], it is important to note that, in the present work, the fractions obtained by differential centrifugation are defined as extracellular vesicle-enriched populations (EVEPs). This is stated to emphasize that the samples analyzed were processed with the purpose of obtaining a heterogeneous set enriched in extracellular vesicles of different origin and size. The objective of this study is twofold: to contribute to the immunophenotypic characterization of extracellular vesicles in 'EVEPs samples' for the diagnosis of ALL, and to describe the presence of double-positive $CD3^+CD19^+$ EVs.

2. Materials and Methods

2.1. Patient and Control Samples

A descriptive study was conducted that included adult patients (≥18 years) with a confirmed diagnosis of B-ALL, established according to the criteria of the World Health Organization [19,25,50]. A total of twelve individuals were enrolled in this study. The primary analysis included eight adult patients with B-ALL and three healthy controls (volunteer donors matched for age and sex). One patient with T-ALL served instead as a control to verify the specificity of the assay (Supplementary Materials, Figure S1). The study was approved by the ethics, biosafety, and research committees of the Hospital Regional de Alta Especialidad de Ixtapaluca (protocol NR-053-2024), and all participants signed written informed consent prior to inclusion.

For the CIP diagnosis of patients with B-ALL (n = 8), four had a clinical diagnosis established from BM samples and the remaining four from PB. In patients diagnosed through BM, plasma was obtained as part of the procedure, and an additional 5 mL sample of PB was collected in EDTA tubes. Based on this design, four samples of EVEPs from BM and eight EVEPs from PB were analyzed. In the case of healthy controls, a venous PB sample was obtained in EDTA tubes. Plasma was obtained from all samples; a fraction was processed immediately for flow cytometry analysis, while the rest was stored at −80 °C until later use in confocal microscopy studies.

2.2. Isolation of EVEPs

To obtain the enriched mixture of large and small EVs, which we refer to as EVEPs, these were obtained using a differential centrifugation protocol, introducing modifications to previously described methodologies [31,51]. Briefly, the plasma was initially centrifuged at 400× g for 10 min to remove intact cells, followed by a second centrifugation of the supernatant at 1500× g for 10 min to remove larger cell debris and remnants. Finally, the resulting supernatant was centrifuged at 14,000× g for 15 min at 4 °C, obtaining a pellet corresponding to EVEPs. The pellet was resuspended in pre-filtered 1X PBS and used for subsequent analyses. Given the method used, the events analyzed are consistently described as EVEPs.

2.3. Immunophenotype of EVEPs

The immunophenotypic characterization of EVEPs was performed using the Cyteck Northern Lights-VBR cytometer (Cytek Biosciences, Inc., Fremont, CA 94538, USA). SpectroFlo software, version 3.3.0, was used for acquisition (12282023). EVEPs were identified using a panel of antibodies that included CD63-PE (Sony Part: 2365020, Lot: 215779, clone: H5C6. Sony Biotechnology Inc., San Jose, CA 95112, USA), CD9-PerCP-Cy5.5 (BioLegend, San Diego, CA 92121, USA. Cat: 312110, Lot: B393332, clone H19a.), and CD81-Alexa Fluor 700 (BioLegend Cat: 349518, Lot: B401697, clone 5A6). In parallel, a multicolor panel (cocktail) was used to characterize the clinical leukemic immunophenotype, including antibodies directed against CD45, CD34, CD19, CD10, CD5, CD38, CD20, CD138, CD8,

CD4, CD3, CD7, CD14, CD117, and CD27. All of these were conjugated with fluorochromes compatible with spectral cytometry (BioLegend Cat: 900009158, Lot: B425396).

Prior to use, all antibodies were centrifuged at 14,000× *g* for 15 min to remove any aggregates that could interfere with the analysis of submicrometric particles. The samples were then incubated with the corresponding antibodies for 20 min at room temperature, protected from light. After incubation, they were washed with 1 mL of pre-filtered (0.22 µm) 1X PBS, followed by centrifugation at 14,000× *g* for 15 min at 4 °C. Data were acquired using standardized instrument parameters: FSC = 10, SSC = 10, SSC-B = 115, threshold = 50,000, and signal amplification factor (ASF) = 1. Subsequent data analysis was performed using Kaluza software (version 3.2).

Lysed EVEPs were controlled using detergent (detergent disruption control). EVEP samples were treated with 1% Tween 20 for 30 min at 4 °C to destabilize the lipid membranes. The samples were then processed in the same way as the rest of the assays, including incubation with antibodies, washing, and data acquisition under the same instrumental conditions. Unstained samples were also used to establish the negative regions in the histograms. A control consisting of unfiltered 1X PBS to which antibodies were added without prior centrifugation was also included. All assays were performed in triplicate.

2.4. Confocal Microscopy of EVEPs

For confocal microscopy studies, the samples were thawed at room temperature, continuously, and the EVEP pellet was fixed with 3% paraformaldehyde for one hour. After this time, the samples were washed with 1 mL of PBS by centrifugation at 12,000× *g* for 10 min. The vesicles were blocked with 10% fetal bovine serum for one hour, after which additional washes were performed with 1X PBS. Labeling was performed using CD63-FITC antibodies (BioLegend, Cat: 353006, Lot: B262101), CD19-PerCP-Vio700 (Milteny Biotec, Bergisch Gladbach, Germany, Cat: 130-113-171, clone: LT19) and CD3-PE (Milteny Biotec, Cat: 130-113-131, clone: BW264/56) antibodies. The samples were incubated for 24 h, then washed with 1X PBS and centrifuged three times at 10,000× *g* for 15 min. Once the washing was complete, the supernatant was removed, leaving approximately 30 µL of 1X PBS; a 1:1 concentration of Vectashield antifade mounting medium (Vectashield®, Newark, CA 94560, USA) was added, and the samples were mounted on untreated coverslips. The samples were analyzed on an Axio Imager Z2 LMS900 confocal microscope (Carl Zeiss, Aalen, Germany) using a 63X objective. The analysis was performed using ZEN software version 3.11.105.05000, while the morphometric analysis of the vesicles was performed using Fiji version 1.54p with the EVAnalyzer v8.2.3 plugin (threshold: MaxEntropy; circularity: 0.5–0.9; particle size 0.3–0.5 µm, Z-plane projection: max). The colocalization of fluorescent signals was evaluated using the JACoP v2.1.4 plugin.

2.5. Statistical Analysis

Descriptive statistics were performed, calculating the mean, standard deviation, and 95% confidence interval. Subsequently, for the study population size, an inferential analysis was performed using the Kruskal–Wallis test (regardless of whether some variables met normality criteria). The Dunn test was used for post hoc comparisons of the leukemic immunophenotype. In all cases, a p-value < 0.05 was considered statistically significant. The statistical software used was Sigma Plot 15 Build 15.0.0.13.

Pearson's correlation coefficient (r) was used to calculate colocalization using Fiji software and the JACoP v2.1.4 plugin. The presence of EVs with $CD3^{+}CD19^{+}$ labeling was confirmed with the EVAnalyzer plugin.3.

3. Results

3.1. Clinical Information

Healthy controls were used to standardize the technique, from which 5 mL of PB was obtained. Samples were collected from 12 individuals (7 men, 5 women; mean age of 33.8 years; old range: 18–66 years). The study cohort comprised 8 patients with B-ALL and 3 healthy controls. The remaining patient, diagnosed with T-ALL, was used as a specificity control to confirm the absence of lineage overlap (see Supplementary Materials Figure S1) and was not included in the statistical comparisons of the B-ALL group. All patients included were diagnosed using flow cytometry, molecular biology, and a comprehensive medical diagnosis. Diagnostic analyses were carried out primarily using BM or BP, from which whole blood was obtained; the leukocytes were then isolated from the leukocyte layer. Additionally, two patients with B-ALL had molecular alterations associated with intermediate and high risk, specifically the translocation t(9;22) (q34;q11.2), with a minor breakpoint corresponding to the p190 BCR::ABL1 (e1a2) transcript.

3.2. Standardization of EVEP Analysis by Flow Cytometry

The characterization of EVEPs was performed by spectral flow cytometry. All assays were performed in triplicate (n = 3) to evaluate the reproducibility of the analytical procedure. Reference beads were used to determine the observed sizes and to demonstrate the range of sizes of the EVEPs (Supplementary Materials Figure S2).

Figure 1A shows the analysis strategy, which initially included a time gate (Time) versus lateral dispersion in height (SSC-H), allowing unstable acquisition periods and instrumental artifacts to be excluded. Subsequently, a compatible region for EVEPs was defined. For this purpose, two instrumental configurations were evaluated, and the one that allowed for better event resolution was finally selected: FSC = 10, SSC = 10, SSC-B = 115 threshold = 50,000, and signal amplification factor (ASF) = 1. Similarly, positive regions were established for the tetraspanins CD81, CD63, and CD9, with clearly defined positive populations for these markers observed through histogram analysis. Figure 1B shows the unstained samples as a negative reference for the delimitation of positive regions. Furthermore, the region established as the 10^4 criterion was identified as a positive signal area.

Figure 1C shows signal loss in samples treated with 1% Tween 20 (disruption control) for the tetraspanins evaluated, confirming the viability of the isolation method. Additionally, Figure 1D included a control consisting of unfiltered 1X PBS incubated with antibodies without prior centrifugation, in which a positive signal was detected for CD9 and CD63. These results suggest the methodological importance of not omitting centrifugation before using antibodies.

3.3. Comparison of the Expression of Tetraspanins Associated with Extracellular Vesicles Between Patients with B-ALL and Controls

Once the analysis strategy had been standardized, a comparison was made of the percentage expression of CD9, CD63, and CD81 tetraspanins in EVEPs obtained from patients with B-ALL (BM, white bars; PB, gray bars) and healthy donors (hatched bars), as shown in Figure 2.

Statistical analysis showed no significant differences in the expression of CD81 (H = 3.467, p = 0.196), CD63 (H = 3.289, p = 0.232), or CD9 (H = 5.067, p = 0.086) between the groups evaluated. Despite this, a trend toward lower CD9 expression was observed in BM EVEPs from patients with B-ALL compared to healthy controls. The percentage of CD81 and CD63 expression appears to show a slight tendency to be higher in PB EVEPs from patients with B-ALL compared to the healthy group, without being close to showing a

significant difference. The above result suggests that the three markers evaluated do not constitute a differential marker of malignancy by themselves.

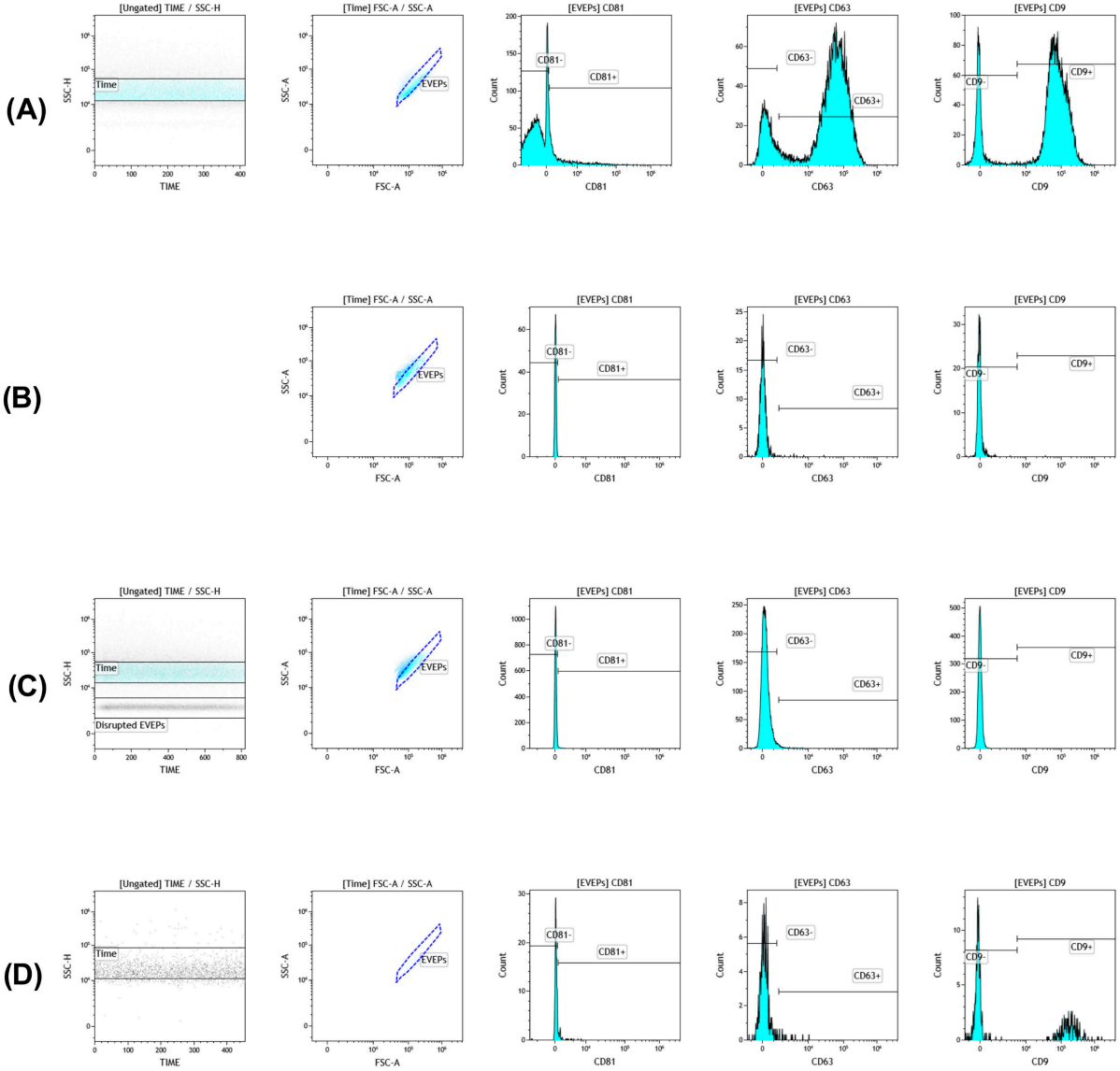


Figure 1. Standardization of the analysis of extracellular vesicle-enriched populations using spectral flow cytometry. The phenotypic characterization of EVEPs is described according to the following strategy: (**A**) Cleaning and event selection: A time window (gate) was applied against side scatter (SSC-H) to exclude artifacts and aggregates, subsequently defining a specific region for EVEPs that excludes unwanted particles. (**B**) Control of unstained EVEPs. (**C**) Disruption control (1% Tween 20): In order to confirm that the signal of interest corresponds to EVs and not lysates or soluble antigens, treatment with 1% Tween was performed, observing the absence of positivity events in the histogram after this procedure. (**D**) Noise control—aggregates removed by centrifugation (PBS + antibodies without centrifugation): An unfiltered 1X PBS sample was included to which antibodies were added without prior centrifugation; a positive signal was detected for CD9 and CD63 markers in this control condition. All assays were performed in triplicate, $n = 3$.

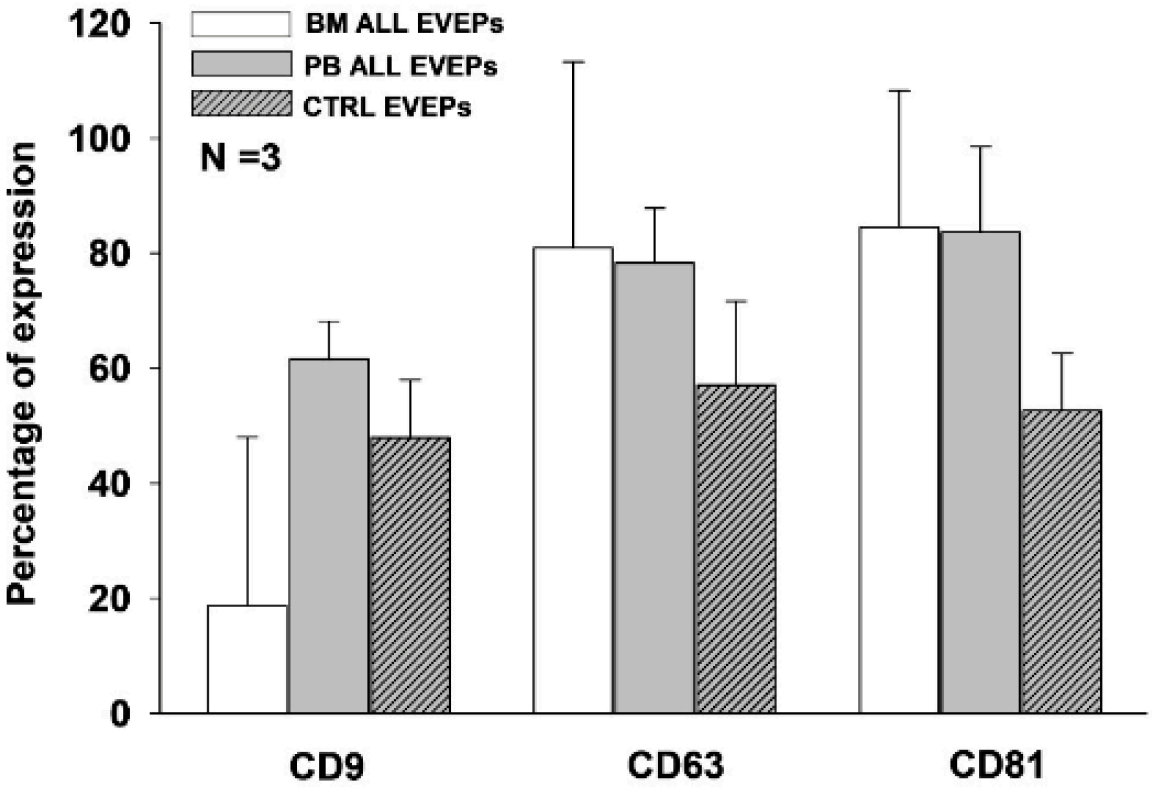
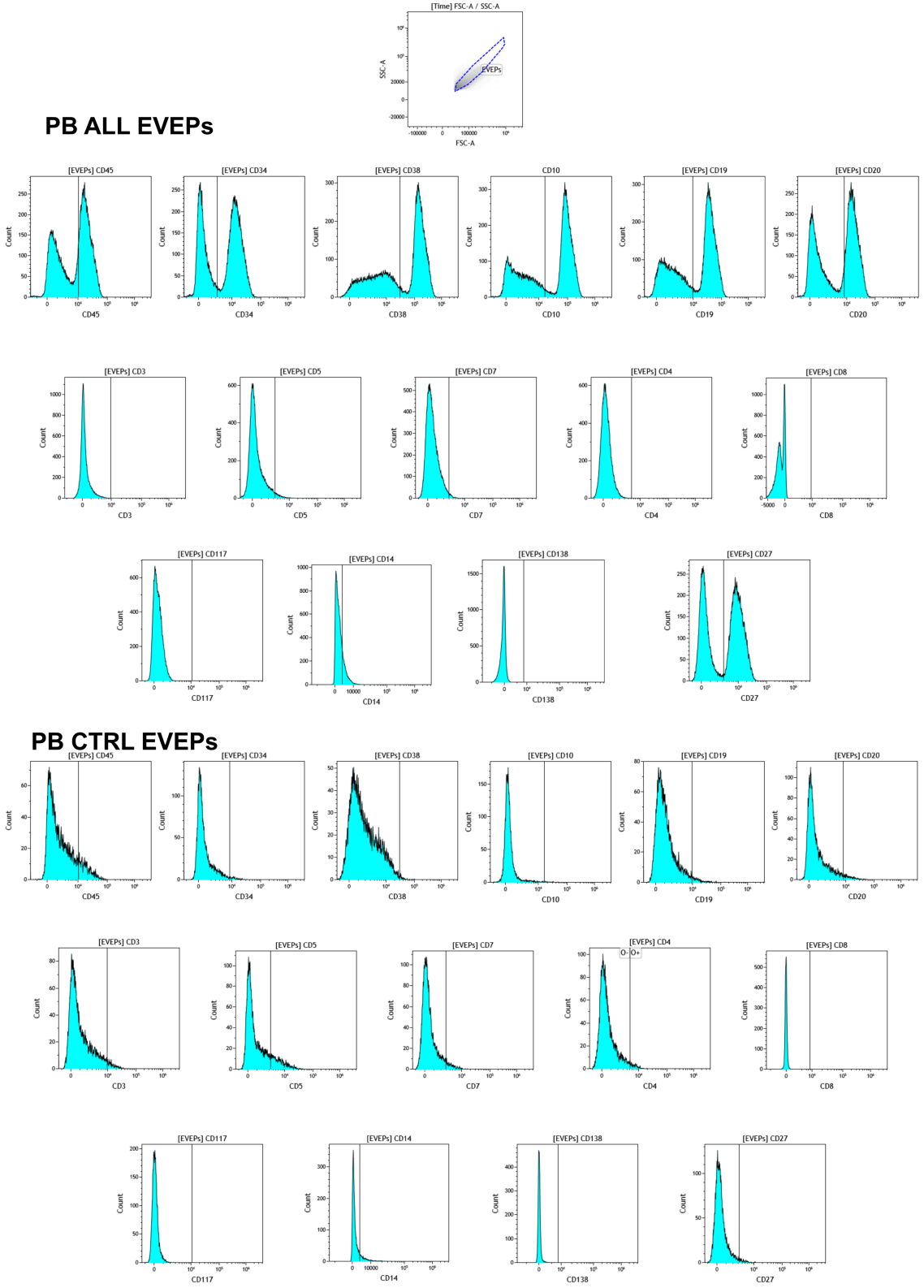


Figure 2. Comparison of the percentage of tetraspanin-positive EVEPs between patients with B-ALL and controls. A comparative analysis of the expression of CD9, CD63, and CD81 markers (EV-associated tetraspanins) was performed by flow cytometry, using histograms for representation. Samples from patients with B-ALL were evaluated, both from bone marrow (white bars) and peripheral blood (gray bar), and compared with those obtained from healthy controls (hatched bars). All tests were performed in triplicate (n = 3). Statistical analysis using the non-parametric Kruskal–Wallis test revealed no statistically significant differences in marker expression between groups for CD81 (H = 3.467, p = 0.196), CD63 (H = 3.289, p = 0.232), or CD9 (H = 5.067, p = 0.086). Standard deviation is shown.

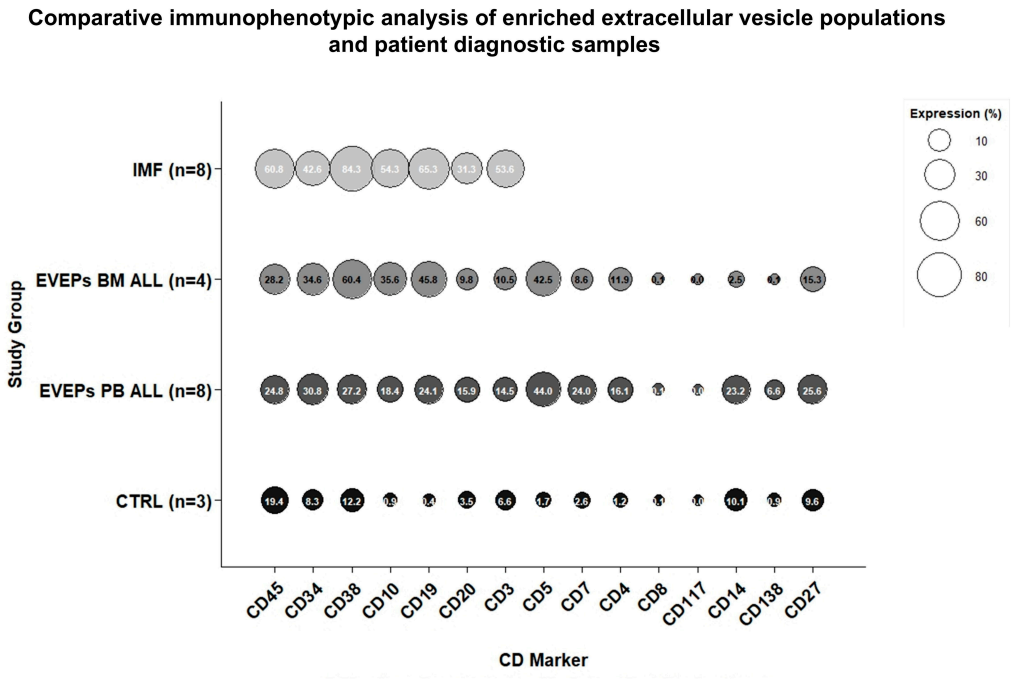
3.4. Immunophenotype of EVEPs and Comparison with Clinical Immunophenotype

Figure 3A shows representative histograms corresponding to EVEPs obtained from PB from a patient with B-ALL and their comparison with a healthy control. These representations show a clear increase in the percentage expression of markers characteristic of the B-cell leukemic lineage, including CD45, CD34, CD38, CD19, CD10, and CD20. Consistently, there was no evidence of overexpression of markers associated with other hematopoietic lineages, such as the T lineage (CD3, CD5, CD7, CD4, CD8, and CD27) or the myeloid lineage (CD14 and CD117), or the plasma cell marker CD138, suggesting a phenotypic specificity of the EVEPs analyzed. The result in Figure 3A suggests that EVEPs can function and be used as a reflection of the tumor cell phenotype, specifically shown in patients with a common B-ALL profile. The ability to detect the $CD10^+/CD19^+/CD34^+/CD38^+$ fingerprint suggests the use of EVEPs as a liquid biopsy from PB and their analysis by flow cytometry.

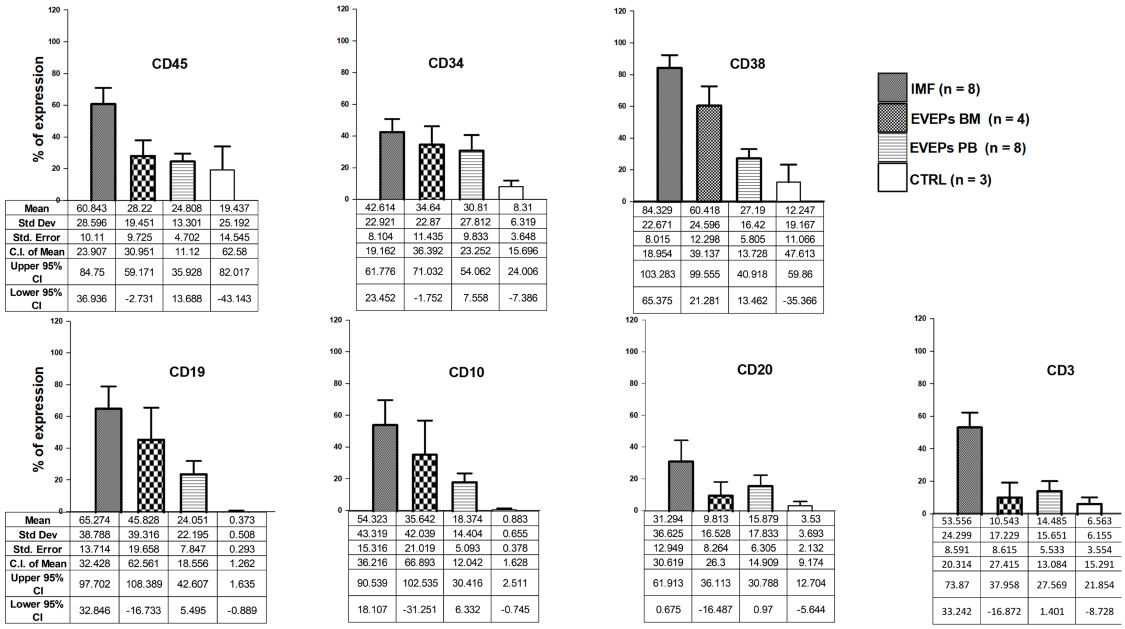


(**A**)

Figure 3. *Cont.*



(**B**)



(**C**)

Figure 3. (**A**) Immunophenotypic comparison of PB EVEPs. Representative histograms showing the immunophenotype of EVEPs obtained from the peripheral blood of a patient with B-cell acute lymphoblastic leukemia (B-ALL) and their comparison with a healthy control (PB CTRL EVEPs). (**B**) Comparative analysis of the expression profile of the marker cocktail in EVEPs. A bubble chart showing the average percentage of expression of CD markers in CIP (n = 8), PB ALL EVEPs (n = 8), BM ALL EVEPs (n = 4), and CTRL (n = 3). Fifteen markers were analyzed: CD45, CD34, CD19, CD10, CD20, CD3, CD38, CD5, CD14, CD8, CD4, CD7, CD27, CD117, and CD138. The bubble size and distribution allow differences to be observed between samples from patients with ALL and CIP vs. the control, including CD38, CD10, CD34, CD19, CD20, and CD5. Kruskal–Wallis analysis followed by Dunn's post hoc test showed a statistically significant difference in CD38 expression, with the CIP group showing higher levels than the control (p = 0.011) and the EVEP PB ALL group

(p = 0.012). In the comparison of all groups, the other markers did not show significant differences using this strategy. (**C**) Quantitative analysis of markers associated with B-ALL in EVEPs representing the average expression percentage with the standard error of selected markers associated with B-cell acute lymphoblastic leukemia in the different groups analyzed. The lower and upper 95% CIs of the mean were calculated. This representation was used to visualize the precision of the estimated mean and explore biological trends between groups based on '*n*'.

Figure 3B shows a visual representation using a bubble chart of the average percentage of marker-positive types included in the analyzed cocktail, comparing four study groups: clinical immunophenotype (CIP, n = 8), bone marrow EVEPs from patients with B-ALL (BM ALL EVEPs, n = 4), peripheral blood EVEPs from patients with B-ALL (PB ALL EVEPs, n = 8), and healthy controls (CTRL, n = 3). The CIP group consists of clinical results from four BM samples and four PB samples. The size of the bubble and the number inside it represent the average percentage of expression. Visually, the B lineage and progenitor markers CD34, CD38, CD19, and CD10 show very high expression in tumor cells (CIP), followed by patient EVEPs (BM ALL and PB ALL), suggesting that EVEPs reflect or inherit the protein signature of the cancer cells from which they originate. In ALL EVEPs, a notable increase in CD5 expression (~42–45%) was observed compared with the control group (1.7%). Statistical analysis was performed using the Kruskal–Wallis test followed by Dunn's post hoc test. The most robust finding was a statistically significant difference in CD38 expression: the CIP group showed higher levels compared with the control group (p = 0.011), and the EVEP group also exhibited higher levels compared with the control group (p = 0.0001), including the PB ALL EVEP subgroup (p = 0.012). The remaining CD markers showed no statistically significant differences between groups. CD45 was the marker most abundantly detected in healthy controls (~15%), which is expected due to its basal expression in EVs as part of immune homeostasis. Its levels increased in EVEPs from PB ALL and BM ALL patients, with mean values of approximately 24% and 28%, respectively.

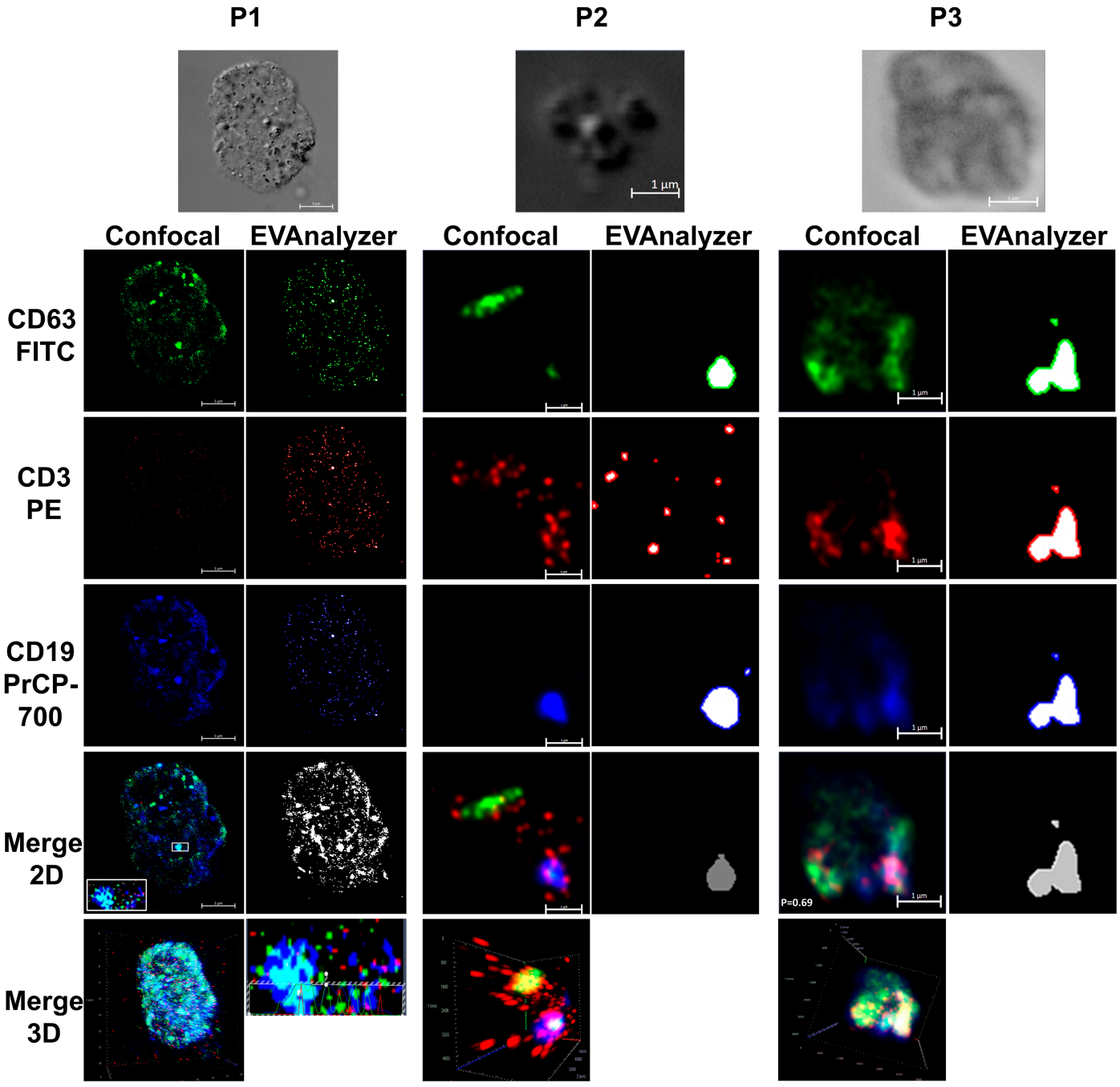
Given the above results, we proceeded to analyze the statistics of the groups in Figure 3C, obtaining the lower and upper 95% CIs of the mean, which showed the absence of overlap in the range of values between several groups of interest, such as CD19 and CD10 between the healthy PB control and the EVEPs of PB B-ALL. The absence of overlap between the ranges of the lower and upper 95% CIs of the mean of the two groups indicates or suggests the existence of a statistically significant difference between them. The statistical findings are consistent with the observed graphical trends.

3.5. Identification of $CD3^+$ $CD19^+$ $CD63^+$ Aggregates Using Confocal Microscopy

Finally, confocal microscopy was used to evaluate EVEPs from the peripheral blood of three patients with B-cell ALL (Figure 4A). The samples were labeled with anti-CD63-FITC, anti-CD3-PE and anti-CD19-PerCP-Vio700 antibodies. Following the EVEP isolation procedure via centrifugation, structures consistent with large multivesicular aggregates, with diameters ranging from approximately 2 to 21 μm, were identified in the B-ALL samples; these aggregates showed a positive signal for CD3, CD19 and CD63. Figure 4 shows one of these EVEP aggregates, where sites of marker colocalization were occasionally observed; consequently, a quantitative analysis of this colocalization was performed, yielding a Pearson correlation coefficient of 0.69 between the CD3 and CD19 signals, a value consistent with partial colocalization of both markers within the same structure (Figure 4A). Concurrently, the circularity of the EVEPs was confirmed using the EVAnalyzer plugin of ImageJ2 software (version 2.3.0). Additionally, a morphometric analysis was performed using the same plugin, applying strict segmentation criteria. A circularity index of $\geq$0.9 and a minimum intensity threshold of 20 were established to ensure an objective selection

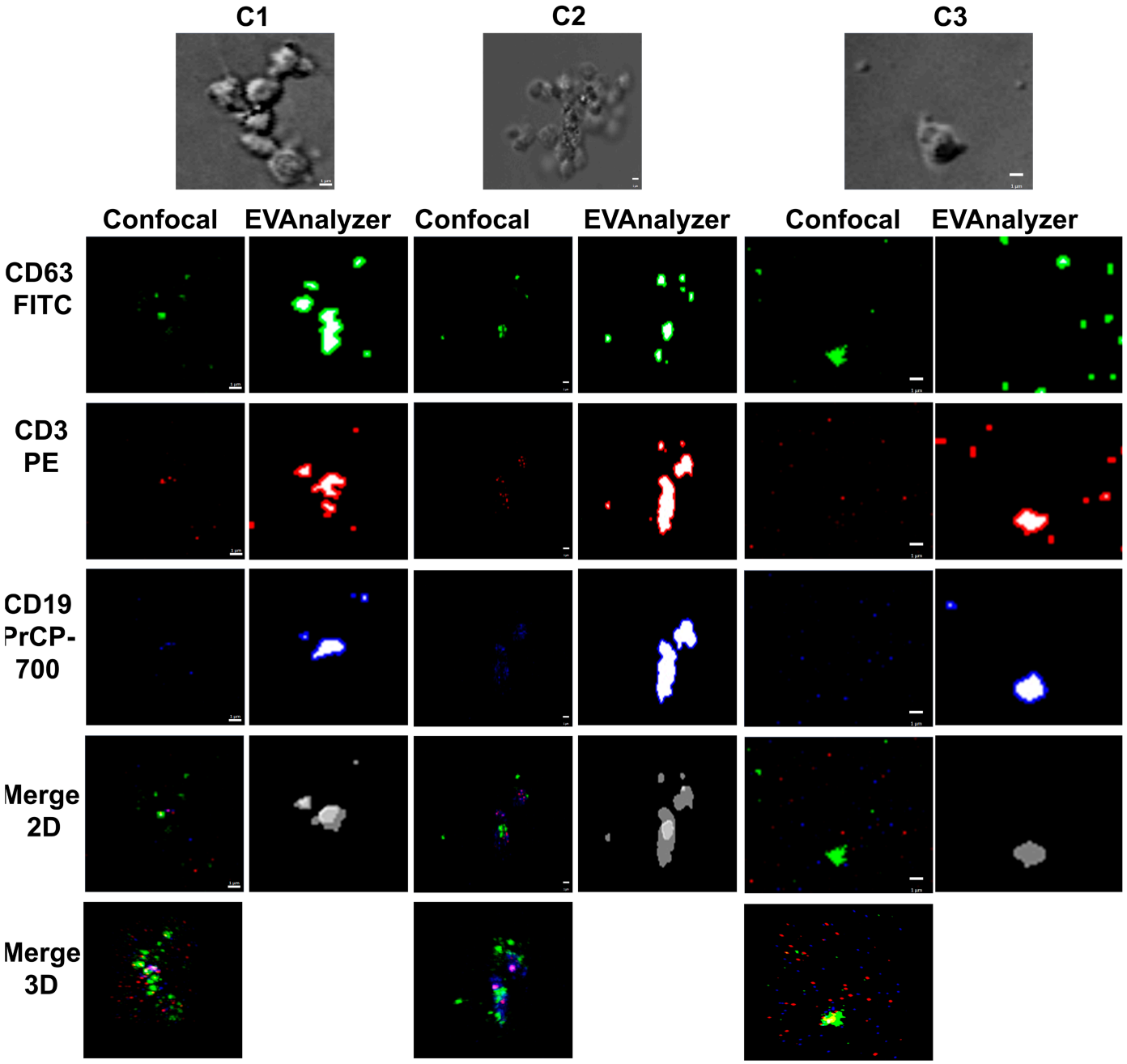
of structures consistent with EVEPs and to minimize the inclusion of artefacts. These parameters confirmed the vesicular morphology of the analyzed structures.

Three samples from apparently healthy individuals were used as a reference (Figure 4B), in which $CD3^{+}CD19^{+}$ double-positive cells were also observed. Upon corroborating this by flow cytometry, a tendency toward a higher percentage of double-positive $CD3^{+}CD19^{+}$ EVEPs was observed in the samples from patients with B-ALL compared with the control samples; however, statistical analysis did not reveal a significant difference (Supplementary Materials Figure S3).



(**A**)

Figure 4. *Cont.*



(**B**)

Figure 4. (**A**) Identification of $CD3^+CD19^+$ EVs in patients with B-ALL from peripheral blood. The different markers were detected in EVEP aggregates, and occasionally EVs double positive for $CD3^+$ and $CD19^+$ in peripheral blood samples from patients (P1, P2, P3) with B-ALL (n = 3). The samples were labeled with anti-CD3-PE, anti-CD19-PerCP-Vio700, and anti-CD63-FITC antibodies. The images were captured using an Axio Imager Z2 microscope (Carl Zeiss) and analyzed using ZEN lite software. Verification of the morphometric and colocalization characteristics specific to EVs was performed using ImageJ2 software and the EVAnalyzer plugin. (**B**) Identification of $CD3^+CD19^+$ EVEPs in controls (C1, C2, C3) from peripheral blood.

4. Discussion

In recent years, extracellular vesicles (EVs) have gained increasing interest as a window into exploring biological processes associated with oncohematological diseases. In the context of leukemia, it has been reported that some malignant cells release EVs capable of transporting proteins, lipids, and nucleic acids, suggesting a possible reflection of both the

tumor state and its interaction with the BM and immune microenvironment [9,29,52–54]. However, the analysis of EVs in complex tissues such as PB remains technically and conceptually challenging due to the coexistence of non-vesicular particles with similar physical–optical properties and the biological heterogeneity inherent to leukemia, which particularly complicates its study in acute lymphoblastic leukemia (ALL) [44,55].

The present study was descriptive and exploratory in nature, aimed at characterizing the immunophenotype of extracellular vesicle-enriched populations (EVEPs) obtained from the BM and PB of adult patients with B-ALL. To this end, spectral flow cytometry and confocal microscopy were used as complementary approaches. From its design, this work focused on documenting expression patterns, apparent discrepancies between compartments, and poorly described events that would provide information on the complexity of the vesicular secretome in this context, so that they could be considered in the development of strategies for analyzing clinical associations, prognostic inferences, or diagnostic applications.

A key limitation of this study is the small size of the final cohort (n = 8 B-ALL and n = 3 controls), which limits the statistical power to detect significant differences using robust multiple comparison tests. This restriction means that the results must be interpreted primarily as consistent biological trends rather than conclusive differences. Additionally, the cross-sectional design prevents the evaluation of dynamic changes associated with disease progression or treatment. These limitations are consistent with other initial exploratory studies in ALL that have addressed the analysis of EVs as a starting point for further research [26,29,54,56]. However, analysis with 95% confidence intervals (95% CIs) revealed groups with a clear separation from the control, suggesting an underlying biological effect that warrants validation in future research, including the dynamics of the expression of markers such as CD3 and CD19 in EVs from ALL patients during disease progression and in response to treatment, with the findings presented here providing a solid exploratory basis.

From a methodological point of view, removing unwanted contaminants at 1500× g and subsequently isolating EVs by differential centrifugation up to 14,000× g allowed us to obtain the EV-enriched fraction, predominantly in larger vesicles (sample obtained in accordance with the purposes of this study), commonly associated with microvesicles, in line with previously reported strategies [31]. This aspect is relevant, since larger EVs tend to have a higher total protein load and, consequently, a higher density of surface antigens, which may favor their detection by flow cytometry. Additionally, the fact that this approach does not require ultracentrifuges or highly specialized equipment represents a key operational advantage that enhances its implementation and reproducibility in conventional clinical settings.

The purpose of this study was to detect ALL-associated markers in the EVEP samples obtained, which was achieved. However, it is important to bear in mind that, according to the recommendations of MISEV2023 [33] and MIBlood-EV [13], this type of isolation does not allow for the complete exclusion of co-isolation of non-vesicular particles, particularly lipoproteins such as LDL (18–25 nm) and VLDL (30–80 nm), which share size ranges and physical–optical properties with the smallest EVs [57]. In PB, the abundance of lipoproteins may be influenced by the patient's metabolic and inflammatory status, so it is suggested that this should be taken into account in studies where it could have a drastic influence, such as in studies focused on the smallest EVs [58,59]. For this reason, together with the variety of EVs obtained, the term EVEPs is deliberately used throughout the study, referring to a set of large and small EVs, avoiding the assumption that all detected events correspond exclusively to extracellular vesicles.

In order to carry out a technical validation of the spectral flow cytometry detection analysis, specificity controls were added, including tetraspanins (CD9, CD63, and CD81), unstained samples, controls with 1% Tween, and PBS with antibodies without prior centrifugation. These controls support the membranous nature of the events analyzed, reducing limitations in complex biological matrices, thereby seeking rigor and consistency with established guidelines [60]. It is important to note that, although we did not find a sufficient statistical difference, our results are consistent with those presented by Li et al. 2022 [61].

All validation experiments were performed in triplicate to improve reproducibility, optimize selection strategies and ensure consistency in the detection of EVEPs. However, despite these technical advantages, the biological variability inherent in human samples represents a significant limitation. As in clinical diagnostic settings, EVEP profiles can vary significantly between individuals due to underlying biological and pathological heterogeneity. Therefore, whilst triplicate measurements enhance technical reliability, they do not fully account for inter-sample variability, underscoring the need for larger cohorts to validate and generalize these findings.

In the global analysis of markers, CD38 showed very high expression in patient ALL samples, sufficient to show a statistically significant difference after non-parametric analysis of the heterogeneous cohort groups (n between 3 and 8 per group). This behavior is consistent with the role of CD38 as a widely described activation marker in B-ALL [62–64]. In contrast, when viewing the graphs of classic B-lineage markers (CD19, CD10, and CD20), these appear to show relative attenuation in the peripheral EV compartment when compared to the cellular immunophenotype. This phenomenon could be interpreted as a 'dilution' of the B lineage in circulating EVs, suggesting that liquid biopsy strategies based exclusively on these markers may require correlation or normalization factors to avoid underestimating tumor burden. However, it is essential to emphasize that direct comparison between cellular and vesicular histograms has intrinsic limitations. Even so, when comparing EVs from patients with B-ALL versus healthy donors, a clear trend toward higher expression of B markers was observed in the leukemic context, indicating that the vesicular compartment retains relevant biological information and is consistent with other studies [26,61,65].

In the samples we analyzed using immunostaining, we found EVs with the presence of markers typically associated with the T lineage (CD3, CD5, CD7, and CD4) in EVEPs from patients with B-ALL. The literature documents a constitutive basal secretion that is 'low constitutive basal secretion of small T-cell EVs' in healthy donors [66–68], which would explain the presence of these EVs in the total EVEPs of patients. It is important to note that the bloodstream contains EVs of all cell types that secrete them, including those with the B-ALL signature. Furthermore, the finding of EVs of different origins can be explained by several non-mutually exclusive mechanisms: aggregation of EVs of different origins, interactions between tumor EVs and EVs derived from activated immune cells, or the release of EVs by non-neoplastic populations secreted constitutively or by stimulation in the leukemic microenvironment.

When we precipitated EVEPs by centrifugation and subsequently processed them for confocal microscopy, we observed, on a qualitative basis, that a greater number of EVEP aggregates remained in samples from patients with B-ALL. Confocal microscopy revealed the presence of large (2–21 µm) $CD3^+$ $CD19^+$ $CD63^+$ multivesicular aggregates, in which some EVs co-expressed the $CD3^+$ CD19 markers, as verified by ImageJ2 software colocalization analysis, and confirmation of the presence of some EVs with colocalization using the EVAnalyzer plugin, suggesting that a fraction of the detected events correspond to aggregated structures rather than individual vesicles and, notably, to a lesser frequency of EVs that did possess colocalization. This finding is relevant when considering the possible

involvement of lipoproteins and apolipoproteins in vesicular aggregation. Previous studies have documented an increase in apolipoproteins in patients with B-ALL, as well as their ability to interact with lipid membranes and extracellular particles [45,58,69–71]. In this regard, it is plausible that circulating apolipoproteins contribute to the recruitment and aggregation of EVs from different lineages, promoting the formation of vesicular complexes capable of transporting biological signals that may appear discordant. In this context, evidence of $CD3^+CD19^+$ cell populations in humans is particularly relevant [34], where a subpopulation of $CD3^+CD19^+$ lymphocytes was described, present in both healthy donors and cancer patients, with a significantly higher frequency in the latter. Although this study focuses on cells and not on EVs, it demonstrates that the co-expression of B and T markers is a real biological phenomenon and not a technical artifact, reinforcing the biological plausibility of detecting similar hybrid signatures in the vesicular compartment and EVs.

The specificity of the resulting immunophenotype ($CD3^+CD19^+$) could suggest a degree of selectivity, opening the door to research into its biological role in ALL. It is known that EVs can carry complete functional protein complexes, including those involving membrane receptors [53,72]. It is plausible that EVs derived from B lymphoblasts ($CD19^+$) express immunoregulatory ligands (such as MHC class II molecules), which could be recognized by components of the TCR/CD3 complex present in EVs derived from $CD4^+$ T lymphocytes [44]. This specific interaction would create a targeted molecular bridge, mimicking the initial events of immune synapse formation on a nanometric scale. Although this possibility requires direct validation, it would establish these aggregates as biologically significant entities that reflect cross-lineage communication in the leukemic niche.

It has been suggested that a portion of the double-positive $CD3^+CD19^+$ EVs may be directly secreted by the rare cells that are also double-positive, adding to those vesicles that could originate through post-secretion aggregation mechanisms and possible fusion between EVs [72,73]. Research into fusion between EVs and EV-EV relationships can currently be considered emerging. In mixed-lineage ALL, the presence of double-positive cell populations with concomitant expression of CD3 and CD19 has been documented. Circulating apolipoproteins contribute similarly. Liu et al. 2020 described the existence of B-T cells ($CD19^+CD3^+$) in the peripheral blood of healthy individuals and cancer patients. Although present in both groups, their frequency was significantly higher in cancer patients compared to healthy donors [34]. Other researchers have reported $CD3^+CD19$ cells [74]. Although this hypothesis remains speculative, it offers a conceptual framework for interpreting the observation of multivesicular aggregates and mixed immunophenotypic profiles in the context of leukemia.

It is important to note the limitations inherent in the confocal microscopy used in this study, whose lateral resolution is limited to approximately 180 nm. This restriction prevented the direct visualization of smaller individual vesicles, so the analyses were restricted to larger-scale structures.

It is important to note that the release of EVs is a multifactorial process that may be influenced not only by tumor activity, but also by other clinical and physiological conditions, such as infections and inflammation [27,52,66]. In this study, all PB and BM samples were obtained at the time of diagnosis, prior to the initiation of antileukemic therapy, which enables us to interpret the observed EVEP profiles as representative of a baseline disease state.

However, although the patients were diagnosed de novo, detailed clinical information on concomitant conditions was not systematically available. Therefore, we cannot rule out the possibility that factors other than leukemia may have contributed to the observed EVEP profiles.

Furthermore, it has previously been reported that both the concentration and phenotypic composition of EVs can change over time as a result of disease progression or therapeutic intervention [65,75,76].

In this context, the EVEP profiles described here should be interpreted as a single cross-sectional representation of the disease at the time of diagnosis; further longitudinal studies will be required to assess their dynamic behavior and their potential utility in monitoring disease progression and response to treatment.

Finally, the asymmetry in the composition of the cohort (four samples with a CIP of BM and four of PB) constitutes an additional limitation that could influence the interpretation of comparisons between compartments. However, all samples were included as reference points because the CIP represents the diagnostic standard in hematological practice, reflecting a real clinical scenario.

5. Conclusions

This exploratory study presents EVEPs as potential diagnostic tools for adult B-ALL, representing a viable liquid biopsy option, as the results suggest that they may reflect leukemia in peripheral blood. This can be supported by comparison with the CIP that was obtained. On the other hand, the occasional identification of CD3+CD19+ could be associated with leukemic processes in peripheral blood.

Supplementary Materials: The following supporting information can be downloaded at: https://www.mdpi.com/article/10.3390/immuno6020033/s1, Figure S1: Lineage-specific EVEP signatures from bone marrow accurately distinguish B-ALL from T-ALL without marker co-expression; Figure S2: Identification of EVEPs size range using reference beads; Figure S3: Comparison of $CD3^+$ and $CD19^+$ EVEP expression in peripheral blood of B-ALL patients versus healthy controls.

Author Contributions: Conceptualization, supervision, methodology and project administration: M.S.-M. and F.S.-L.; data curation, formal analysis, and writing—original draft preparation: M.A.C.-Z. and F.S.-L.; funding acquisition: M.S.-M.; investigation and visualization: M.A.C.-Z.; resources: G.A.-A.; software: C.E.M.-R.; validation and writing—review and editing: M.S.-M., F.S.-L., C.E.M.-R. and M.H.-R. All authors have read and agreed to the published version of the manuscript.

Funding: Master thesis work of M.A.C.Z At Escuela Superior de Medicina IPN, from which he was the beneficiary of a Master fellowship from SECIHTI Mexico (CVU number: 2047549), and by the Hospital Regional de Alta Especialidad de Ixtapaluca, Health Services of the Mexican Social Security Institute (IMSS-BIENESTAR).

Institutional Review Board Statement: The study was conducted in accordance with the Declaration of Helsinki and was approved by the Research Ethics, Investigation and Biosecurity Committee of the Hospital Regional de Alta Especialidad de Ixtapaluca (protocol code: NR-053-2024 and date of approval: 26 February 2025).

Informed Consent Statement: Informed consent was obtained from all patients and control subjects involved in the study.

Data Availability Statement: The original contributions presented in this study are included in the article/Supplementary Material. Further inquiries can be directed to the corresponding author(s).

Acknowledgments: We thank the Molecular Pathogenesis Laboratory for providing the microscope for image acquisition, and Diana Karina Camarillo for her assistance with sample collection. We also thank the Hospital Regional de Alta Especialidad for providing the reagents used in this study. We extend our special gratitude to Fundación Comparte Vida A.C. for donating the reagents that made these experiments possible, and especially to Clara Gorodezky for her generous guidance, wisdom, and lasting contributions. Her legacy continues to inspire our work.

Conflicts of Interest: The authors declare no conflicts of interest.

Abbreviations

The following abbreviations are used in this manuscript:

ALL	Acute lymphoblastic leukemia
ASF	Signal amplification factor
B-ALL	B-lineage acute lymphoblastic leukemia
BM	Bone marrow
BCR-ABL1	Breakpoint cluster region–Abelson murine leukemia 1
BSA	Bovine serum albumin
CD	Cluster of differentiation
CIP	Clinical immunophenotype
EVEPs	Extracellular vesicle-enriched populations
EVs	Extracellular vesicles
FSC	Forward scatter
LDL	Low-density lipoprotein
MHC	Major histocompatibility complex
MISEV	Minimal Information for Studies of Extracellular Vesicles
PB	Peripheral blood
SSC	Side scatter
SSC-H	Side scatter height
TCR	T-cell receptor
VLDL	Very low-density lipoprotein

References

1. Sedgwick, A.E.; D'Souza-Schorey, C. The Biology of Extracellular Microvesicles. *Traffic* **2018**, *19*, 319–327. [CrossRef] [PubMed]
2. Nguyen, P.H.D.; Le, A.H.; Pek, J.S.Q.; Pham, T.T.; Jayasinghe, M.K.; Do, D.V.; Phung, C.D.; Le, M.T.N. Extracellular Vesicles and Lipoproteins—Smart Messengers of Blood Cells in the Circulation. *J. Extracell. Biol.* **2022**, *1*, e49. [CrossRef]
3. Doyle, L.M.; Wang, M.Z. Overview of Extracellular Vesicles, Their Origin, Composition, Purpose, and Methods for Exosome Isolation and Analysis. *Cells* **2019**, *8*, 727. [CrossRef] [PubMed]
4. Meldolesi, J. Exosomes and Ectosomes in Intercellular Communication. *Curr. Biol.* **2018**, *28*, R435–R444. [CrossRef]
5. Cocucci, E.; Meldolesi, J. Ectosomes and Exosomes: Shedding the Confusion between Extracellular Vesicles. *Trends Cell Biol.* **2015**, *25*, 364–372. [CrossRef]
6. Kalluri, R.; McAndrews, K.M. The Role of Extracellular Vesicles in Cancer. *Cell* **2023**, *186*, 1610–1626. [CrossRef]
7. Rezaie, J.; Ahmadi, M.; Ravanbakhsh, R.; Mojarad, B.; Mahbubfam, S.; Shaban, S.A.; Shadi, K.; Berenjabad, N.J.; Etemadi, T. Tumor-Derived Extracellular Vesicles: The Metastatic Organotropism Drivers. *Life Sci.* **2022**, *289*, 120216. [CrossRef] [PubMed]
8. Jeppesen, D.K.; Zhang, Q.; Franklin, J.L.; Coffey, R.J. Extracellular Vesicles and Nanoparticles: Emerging Complexities. *Trends Cell Biol.* **2023**, *33*, 667–681. [CrossRef]
9. Ratajczak, M.Z.; Ratajczak, J. Leukemogenesis Occurs in a Microenvironment Enriched by Extracellular Microvesicles/Exosomes: Recent Discoveries and Questions to Be Answered. *Leukemia* **2024**, *38*, 692–698. [CrossRef]
10. Samii, A.; Razmkhah, F. Transformation of Hematopoietic Stem and Progenitor Cells by Leukemia Extracellular Vesicles: A Step Toward Leukemogenesis. *Stem Cell Rev. Rep.* **2020**, *16*, 1081–1091. [CrossRef]
11. Yamashita, M.; Dellorusso, P.V.; Olson, O.C.; Passegué, E. Dysregulated Haematopoietic Stem Cell Behaviour in Myeloid Leukaemogenesis. *Nat. Rev. Cancer* **2020**, *20*, 365–382. [CrossRef] [PubMed]
12. Johnsen, K.B.; Gudbergsson, J.M.; Andresen, T.L.; Simonsen, J.B. What Is the Blood Concentration of Extracellular Vesicles? Implications for the Use of Extracellular Vesicles as Blood-Borne Biomarkers of Cancer. *Biochim. Biophys. Acta (BBA)—Rev. Cancer* **2019**, *1871*, 109–116. [CrossRef] [PubMed]
13. Lucien, F.; Gustafson, D.; Lenassi, M.; Li, B.; Teske, J.J.; Boilard, E.; von Hohenberg, K.C.; Falcón-Perez, J.M.; Gualerzi, A.; Reale, A.; et al. MIBlood-EV: Minimal Information to Enhance the Quality and Reproducibility of Blood Extracellular Vesicle Research. *J. Extracell. Vesicles* **2023**, *12*, e12385. [CrossRef] [PubMed]
14. Vu, L.T.; Peng, B.; Zhang, D.X.; Ma, V.; Mathey-Andrews, C.A.; Lam, C.K.; Kiomourtzis, T.; Jin, J.; McReynolds, L.; Huang, L.; et al. Tumor-secreted Extracellular Vesicles Promote the Activation of Cancer-associated Fibroblasts via the Transfer of MicroRNA-125b. *J. Extracell. Vesicles* **2019**, *8*, 1599680. [CrossRef]
15. Bebelman, M.P.; Janssen, E.; Pegtel, D.M.; Crudden, C. The Forces Driving Cancer Extracellular Vesicle Secretion. *Neoplasia* **2021**, *23*, 149–157. [CrossRef]

16. Dilsiz, N. Role of Exosomes and Exosomal MicroRNAs in Cancer. *Future Sci. OA* **2020**, *6*, FSO465. [CrossRef]
17. Urabe, F.; Kosaka, N.; Ito, K.; Kimura, T.; Egawa, S.; Ochiya, T. Extracellular Vesicles as Biomarkers and Therapeutic Targets for Cancer. *Am. J. Physiol.-Cell Physiol.* **2020**, *318*, C29–C39. [CrossRef]
18. Costa-Silva, B.; Aiello, N.M.; Ocean, A.J.; Singh, S.; Zhang, H.; Thakur, B.K.; Becker, A.; Hoshino, A.; Mark, M.T.; Molina, H.; et al. Pancreatic Cancer Exosomes Initiate Pre-Metastatic Niche Formation in the Liver. *Nat. Cell Biol.* **2015**, *17*, 816–826. [CrossRef]
19. Duffield, A.S.; Mullighan, C.G.; Borowitz, M.J. International Consensus Classification of Acute Lymphoblastic Leukemia/Lymphoma. *Virchows Arch.* **2023**, *482*, 11–26. [CrossRef]
20. Arber, D.A.; Orazi, A.; Hasserjian, R.P.; Borowitz, M.J.; Calvo, K.R.; Kvasnicka, H.M.; Wang, S.A.; Bagg, A.; Barbui, T.; Branford, S.; et al. International Consensus Classification of Myeloid Neoplasms and Acute Leukemias: Integrating Morphologic, Clinical, and Genomic Data. *Blood* **2022**, *140*, 1200–1228. [CrossRef] [PubMed]
21. Harris, M.H.; Czuchlewski, D.R.; Arber, D.A.; Czader, M. Genetic Testing in the Diagnosis and Biology of Acute Leukemia. *Am. J. Clin. Pathol.* **2019**, *152*, 322–346. [CrossRef]
22. Estey, E.H. Acute Myeloid Leukemia: 2019 Update on Risk-Stratification and Management. *Am. J. Hematol.* **2018**, *93*, 1267–1291. [CrossRef] [PubMed]
23. De Kouchkovsky, I.; Abdul-Hay, M. Acute Myeloid Leukemia: A Comprehensive Review and 2016 Update. *Blood Cancer J.* **2016**, *6*, e441. [CrossRef]
24. Malard, F.; Mohty, M. Acute Lymphoblastic Leukaemia. *Lancet* **2020**, *395*, 1146–1162. [CrossRef]
25. Polyatskin, I.L.; Artemyeva, A.S.; Krivolapov, Y.A. Revised WHO Classification of Tumors of Hematopoietic and Lymphoid Tissues 2017 (4th Edition): Lymphoid Tumors. *Arkhiv Patol.* **2019**, *81*, 59. [CrossRef] [PubMed]
26. Miljkovic-Licina, M.; Arraud, N.; Zahra, A.D.; Ropraz, P.; Matthes, T. Quantification and Phenotypic Characterization of Extracellular Vesicles from Patients with Acute Myeloid and B-Cell Lymphoblastic Leukemia. *Cancers* **2021**, *14*, 56. [CrossRef]
27. Kumar, M.A.; Baba, S.K.; Sadida, H.Q.; Al Marzooqi, S.; Jerobin, J.; Altemani, F.H.; Algehainy, N.; Alanazi, M.A.; Abou-Samra, A.-B.; Kumar, R.; et al. Extracellular Vesicles as Tools and Targets in Therapy for Diseases. *Signal Transduct. Target. Ther.* **2024**, *9*, 27. [CrossRef] [PubMed]
28. Longjohn, M.N.; Hudson, J.-A.B.J.; Peña-Castillo, L.; Cormier, R.P.J.; Hannay, B.; Chacko, S.; Lewis, S.M.; Moorehead, P.C.; Christian, S.L. Extracellular Vesicle Small RNA Cargo Discriminates Non-Cancer Donors from Pediatric B-Lymphoblastic Leukemia Patients. *Front. Oncol.* **2023**, *13*, 1272883. [CrossRef]
29. Trino, S.; Lamorte, D.; Caivano, A.; De Luca, L.; Sgambato, A.; Laurenzana, I. Clinical Relevance of Extracellular Vesicles in Hematological Neoplasms: From Liquid Biopsy to Cell Biopsy. *Leukemia* **2021**, *35*, 661–678. [CrossRef]
30. Théry, C.; Witwer, K.W.; Aikawa, E.; Alcaraz, M.J.; Anderson, J.D.; Andriantsitohaina, R.; Antoniou, A.; Arab, T.; Archer, F.; Atkin-Smith, G.K.; et al. Minimal Information for Studies of Extracellular Vesicles 2018 (MISEV2018): A Position Statement of the International Society for Extracellular Vesicles and Update of the MISEV2014 Guidelines. *J. Extracell. Vesicles* **2018**, *7*, 1535750. [CrossRef]
31. Menck, K.; Bleckmann, A.; Schulz, M.; Ries, L.; Binder, C. Isolation and Characterization of Microvesicles from Peripheral Blood. *J. Vis. Exp.* **2017**, *6*, 55057. [CrossRef]
32. Parolini, I.; Federici, C.; Raggi, C.; Lugini, L.; Palleschi, S.; De Milito, A.; Coscia, C.; Iessi, E.; Logozzi, M.; Molinari, A.; et al. Microenvironmental PH Is a Key Factor for Exosome Traffic in Tumor Cells. *J. Biol. Chem.* **2009**, *284*, 34211–34222. [CrossRef]
33. Welsh, J.A.; Goberdhan, D.C.I.; O'Driscoll, L.; Buzas, E.I.; Blenkiron, C.; Bussolati, B.; Cai, H.; Di Vizio, D.; Driedonks, T.A.P.; Erdbrügger, U.; et al. Minimal Information for Studies of Extracellular Vesicles (MISEV2023): From Basic to Advanced Approaches. *J. Extracell. Vesicles* **2024**, *13*, e12404. [CrossRef] [PubMed]
34. Liu, Y.; Ye, S.; Guo, X.; Li, W.; Xia, Y.; Wen, X.; Yu, J.; Jia, Y.; Liu, X.; Guo, Y.; et al. Discovery and Characteristics of B Cell-like T Cells: A Potential Novel Tumor Immune Marker? *Immunol. Lett.* **2020**, *220*, 44–50. [CrossRef]
35. Sódar, B.W.; Kittel, Á.; Pálóczi, K.; Vukman, K.V.; Osteikoetxea, X.; Szabó-Taylor, K.; Németh, A.; Sperlágh, B.; Baranyai, T.; Giricz, Z.; et al. Low-Density Lipoprotein Mimics Blood Plasma-Derived Exosomes and Microvesicles during Isolation and Detection. *Sci. Rep.* **2016**, *6*, 24316. [CrossRef]
36. Jimenez, D.E.; Tahir, M.; Faheem, M.; Alves, W.B.d.S.; Correa, B.d.L.; Andrade, G.R.d; Larsen, M.R.; Oliveira, G.P.d.; Pereira, R.W. Comparison of Four Purification Methods on Serum Extracellular Vesicle Recovery, Size Distribution, and Proteomics. *Proteomes* **2023**, *11*, 23. [CrossRef]
37. Rubinstein, E.; Théry, C.; Zimmermann, P. Tetraspanins Affect Membrane Structures and the Trafficking of Molecular Partners: What Impact on Extracellular Vesicles? *Biochem. Soc. Trans.* **2025**, *53*, 371–382. [CrossRef] [PubMed]
38. Mathieu, M.; Névo, N.; Jouve, M.; Valenzuela, J.I.; Maurin, M.; Verweij, F.J.; Palmulli, R.; Lankar, D.; Dingli, F.; Loew, D.; et al. Specificities of Exosome versus Small Ectosome Secretion Revealed by Live Intracellular Tracking of CD63 and CD9. *Nat. Commun.* **2021**, *12*, 4389. [CrossRef]

39. Kalina, T.; Fišer, K.; Pérez-Andrés, M.; Kuzílková, D.; Cuenca, M.; Bartol, S.J.W.; Blanco, E.; Engel, P.; van Zelm, M.C. CD Maps—Dynamic Profiling of CD1–CD100 Surface Expression on Human Leukocyte and Lymphocyte Subsets. *Front. Immunol.* **2019**, *10*, 2434. [CrossRef]
40. Kumar, J.; Khan, A.A.; Saraf, A.; Bhargava, M. Expression of CD20 in B Cell Precursor Acute Lymphoblastic Leukemia. *Indian J. Hematol. Blood Transfus.* **2014**, *30*, 16–18. [CrossRef] [PubMed]
41. Blatt, K.; Menzl, I.; Eisenwort, G.; Cerny-Reiterer, S.; Herrmann, H.; Herndlhofer, S.; Stefanzl, G.; Sadovnik, I.; Berger, D.; Keller, A.; et al. Phenotyping and Target Expression Profiling of CD34+/CD38− and CD34+/CD38+ Stem- and Progenitor Cells in Acute Lymphoblastic Leukemia. *Neoplasia* **2018**, *20*, 632–642. [CrossRef]
42. Japp, A.S.; Meng, W.; Rosenfeld, A.M.; Perry, D.J.; Thirawatananond, P.; Bacher, R.L.; Liu, C.; Gardner, J.S.; Atkinson, M.A.; Kaestner, K.H.; et al. TCR+/BCR+ Dual-Expressing Cells and Their Associated Public BCR Clonotype Are Not Enriched in Type 1 Diabetes. *Cell* **2021**, *184*, 827–839.e14. [CrossRef]
43. Zhang, Y.; Guo, C.; Zhou, Y.; Zhang, W.; Zhu, Z.; Wang, W.; Wan, Y. A Biphenotypic Lymphocyte Subset Displays Both T- and B-Cell Functionalities. *Commun. Biol.* **2024**, *7*, 28. [CrossRef]
44. Buzás, E.I.; Tóth, E.Á.; Sódar, B.W.; Szabó-Taylor, K.É. Molecular Interactions at the Surface of Extracellular Vesicles. *Semin. Immunopathol.* **2018**, *40*, 453–464. [CrossRef]
45. Tóth, E.Á.; Turiák, L.; Visnovitz, T.; Cserép, C.; Mázló, A.; Sódar, B.W.; Försönits, A.I.; Petővári, G.; Sebestyén, A.; Komlósi, Z.; et al. Formation of a Protein Corona on the Surface of Extracellular Vesicles in Blood Plasma. *J. Extracell. Vesicles* **2021**, *10*, e12140. [CrossRef]
46. Alexander, T.B.; Gu, Z.; Iacobucci, I.; Dickerson, K.; Choi, J.K.; Xu, B.; Payne-Turner, D.; Yoshihara, H.; Loh, M.L.; Horan, J.; et al. The Genetic Basis and Cell of Origin of Mixed Phenotype Acute Leukaemia. *Nature* **2018**, *562*, 373–379. [CrossRef]
47. Johnson, S.M.; Dempsey, C.; Parker, C.; Mironov, A.; Bradley, H.; Saha, V. Acute Lymphoblastic Leukaemia Cells Produce Large Extracellular Vesicles Containing Organelles and an Active Cytoskeleton. *J. Extracell. Vesicles* **2017**, *6*, 1294339. [CrossRef]
48. Al-Nedawi, K.; Meehan, B.; Micallef, J.; Lhotak, V.; May, L.; Guha, A.; Rak, J. Intercellular Transfer of the Oncogenic Receptor EGFRvIII by Microvesicles Derived from Tumour Cells. *Nat. Cell Biol.* **2008**, *10*, 619–624. [CrossRef] [PubMed]
49. Abdulmawjood, B.; Roma-Rodrigues, C.; Fernandes, A.R.; Baptista, P.V. Liquid Biopsies in Myeloid Malignancies. *Cancer Drug Resist.* **2019**, *2*, 1044–1061. [CrossRef] [PubMed]
50. Arber, D.A.; Orazi, A.; Hasserjian, R.; Thiele, J.; Borowitz, M.J.; Le Beau, M.M.; Bloomfield, C.D.; Cazzola, M.; Vardiman, J.W. The 2016 Revision to the World Health Organization Classification of Myeloid Neoplasms and Acute Leukemia. *Blood* **2016**, *127*, 2391–2405. Erratum in *Blood* **2016**, *128*, 462–463. https://doi.org/10.1182/blood-2016-06-721662. [CrossRef] [PubMed]
51. Sierra-López, F.; Iglesias-Vazquez, V.; Baylon-Pacheco, L.; Ríos-Castro, E.; Osorio-Trujillo, J.C.; Lagunes-Guillén, A.; Chávez-Munguía, B.; Hernández, S.B.; Acosta-Altamirano, G.; Talamás-Rohana, P.; et al. A Fraction of Escherichia Coli Bacteria Induces an Increase in the Secretion of Extracellular Vesicle Polydispersity in Macrophages: Possible Involvement of Secreted EVs in the Diagnosis of COVID-19 with Bacterial Coinfections. *Int. J. Mol. Sci.* **2025**, *26*, 3741. [CrossRef] [PubMed]
52. Karami Fath, M.; Azami, J.; Jaafari, N.; Akbari Oryani, M.; Jafari, N.; Poor, A.K.; Azargoonjahromi, A.; Nabi-Afjadi, M.; Payandeh, Z.; Zalpoor, H.; et al. Exosome Application in Treatment and Diagnosis of B-Cell Disorders: Leukemias, Multiple Sclerosis, and Arthritis Rheumatoid. *Cell. Mol. Biol. Lett.* **2022**, *27*, 74. [CrossRef]
53. Ratajczak, J.; Wysoczynski, M.; Hayek, F.; Janowska-Wieczorek, A.; Ratajczak, M.Z. Membrane-Derived Microvesicles: Important and Underappreciated Mediators of Cell-to-Cell Communication. *Leukemia* **2006**, *20*, 1487–1495. [CrossRef]
54. Caivano, A.; Laurenzana, I.; De Luca, L.; La Rocca, F.; Simeon, V.; Trino, S.; D'Auria, F.; Traficante, A.; Maietti, M.; Izzo, T.; et al. High Serum Levels of Extracellular Vesicles Expressing Malignancy-Related Markers Are Released in Patients with Various Types of Hematological Neoplastic Disorders. *Tumor Biol.* **2015**, *36*, 9739–9752. [CrossRef]
55. Yang, H.-Q.; Qiu, F.-Q.; Jin, K.E.; Jiang, N.-G.; Zhang, L.I. High Plasma Levels of Oxidatively Modified Low-Density Lipoproteins Are Associated with the Suppressed Expression of Immunomodulatory Molecules in Patients with Hematological Malignancies. *Exp. Ther. Med.* **2015**, *9*, 2394–2400. [CrossRef]
56. Kwaan, H.; Magalhães Rego, E. Role of Microparticles in the Hemostatic Dysfunction in Acute Promyelocytic Leukemia. *Semin. Thromb. Hemost.* **2010**, *36*, 917–924. [CrossRef]
57. Lozano-Andrés, E.; Enciso-Martinez, A.; Gijsbers, A.; Libregts, S.F.W.M.; Pinheiro, C.; Van Niel, G.; Hendrix, A.; Peters, P.J.; Otto, C.; Arkesteijn, G.J.A.; et al. Physical Association of Low Density Lipoprotein Particles and Extracellular Vesicles Unveiled by Single Particle Analysis. *bioRxiv* **2022**. [CrossRef]
58. Morel, S.; Leahy, J.; Fournier, M.; Lamarche, B.; Garofalo, C.; Grimard, G.; Poulain, F.; Delvin, E.; Laverdière, C.; Krajinovic, M.; et al. Lipid and Lipoprotein Abnormalities in Acute Lymphoblastic Leukemia Survivors. *J. Lipid Res.* **2017**, *58*, 982–993. [CrossRef]
59. Malhotra, J.; Tonorezos, E.S.; Rozenberg, M.; Vega, G.L.; Sklar, C.A.; Chou, J.; Moskowitz, C.S.; Eshelman-Kent, D.A.; Janiszewski, P.; Ross, R.; et al. Atherogenic Low Density Lipoprotein Phenotype in Long-Term Survivors of Childhood Acute Lymphoblastic Leukemia. *J. Lipid Res.* **2012**, *53*, 2747–2754. [CrossRef] [PubMed]

60. Welsh, J.A.; Van Der Pol, E.; Arkesteijn, G.J.A.; Bremer, M.; Brisson, A.; Coumans, F.; Dignat-George, F.; Duggan, E.; Ghiran, I.; Giebel, B.; et al. MIFlowCyt-EV: A Framework for Standardized Reporting of Extracellular Vesicle Flow Cytometry Experiments. *J. Extracell. Vesicles* **2020**, *9*, 1713526. [CrossRef] [PubMed]
61. Li, L.; Görgens, A.; Mussack, V.; Pepeldjiyska, E.; Hartz, A.S.; Rank, A.; Schmohl, J.; Krämer, D.; Andaloussi, S.E.; Pfaffl, M.W.; et al. Description and Optimization of a Multiplex Bead-Based Flow Cytometry Method (MBFCM) to Characterize Extracellular Vesicles in Serum Samples from Patients with Hematological Malignancies. *Cancer Gene Ther.* **2022**, *29*, 1600–1615. [CrossRef] [PubMed]
62. Zhong, X.; Ma, H. Targeting CD38 for Acute Leukemia. *Front. Oncol.* **2022**, *12*, 1007783. [CrossRef]
63. Jiang, Z.; Wu, D.; Lin, S.; Li, P. CD34 and CD38 Are Prognostic Biomarkers for Acute B Lymphoblastic Leukemia. *Biomark. Res.* **2016**, *4*, 23. [CrossRef] [PubMed]
64. Eveillard, M.; Floc'h, V.; Robillard, N.; Debord, C.; Wuilleme, S.; Garand, R.; Rialland, F.; Thomas, C.; Peterlin, P.; Guillaume, T.; et al. CD38 Expression in B-Lineage Acute Lymphoblastic Leukemia, a Possible Target for Immunotherapy. *Blood* **2016**, *128*, 5268. [CrossRef]
65. Magalhães-Gama, F.; Malheiros Araújo Silvestrini, M.; Neves, J.C.F.; Araújo, N.D.; Alves-Hanna, F.S.; Kerr, M.W.A.; Carvalho, M.P.S.S.; Tarragô, A.M.; Soares Pontes, G.; Martins-Filho, O.A.; et al. Exploring Cell-Derived Extracellular Vesicles in Peripheral Blood and Bone Marrow of B-Cell Acute Lymphoblastic Leukemia Pediatric Patients: Proof-of-Concept Study. *Front. Immunol.* **2024**, *15*, 1421036. [CrossRef]
66. Auber, M.; Svenningsen, P. An Estimate of Extracellular Vesicle Secretion Rates of Human Blood Cells. *J. Extracell. Biol.* **2022**, *1*, e46. [CrossRef]
67. Wahlgren, J.; Karlson, T.D.L.; Glader, P.; Telemo, E.; Valadi, H. Activated Human T Cells Secrete Exosomes That Participate in IL-2 Mediated Immune Response Signaling. *PLoS ONE* **2012**, *7*, e49723. [CrossRef]
68. Griesel, L.; Kaleja, P.; Tholey, A.; Lettau, M.; Janssen, O. Comparative Analysis of Extracellular Vesicles from Cytotoxic $CD8^+$ Aβ T Cells and Γδ T Cells. *Cells* **2024**, *13*, 1745. [CrossRef]
69. Lu, C.-W.; Lo, Y.-H.; Chen, C.-H.; Lin, C.-Y.; Tsai, C.-H.; Chen, P.-J.; Yang, Y.-F.; Wang, C.-H.; Tan, C.-H.; Hou, M.-F.; et al. VLDL and LDL, but Not HDL, Promote Breast Cancer Cell Proliferation, Metastasis and Angiogenesis. *Cancer Lett.* **2017**, *388*, 130–138. [CrossRef]
70. Oguro, H. The Roles of Cholesterol and Its Metabolites in Normal and Malignant Hematopoiesis. *Front. Endocrinol.* **2019**, *10*, 204. [CrossRef]
71. Goossens, P.; Rodriguez-Vita, J.; Etzerodt, A.; Masse, M.; Rastoin, O.; Gouirand, V.; Ulas, T.; Papantonopoulou, O.; Van Eck, M.; Auphan-Anezin, N.; et al. Membrane Cholesterol Efflux Drives Tumor-Associated Macrophage Reprogramming and Tumor Progression. *Cell Metab.* **2019**, *29*, 1376–1389.e4. [CrossRef] [PubMed]
72. Karmacharya, M.; Kumar, S.; Cho, Y.-K. Tuning the Extracellular Vesicles Membrane through Fusion for Biomedical Applications. *J. Funct. Biomater.* **2023**, *14*, 117. [CrossRef]
73. Morandi, M.I.; Busko, P.; Ozer-Partuk, E.; Khan, S.; Zarfati, G.; Elbaz-Alon, Y.; Abou Karam, P.; Napso Shogan, T.; Ginini, L.; Gil, Z.; et al. Extracellular Vesicle Fusion Visualized by Cryo-Electron Microscopy. *PNAS Nexus* **2022**, *1*, pgac156. [CrossRef] [PubMed]
74. Li, Q.; Wang, J.; Zhang, M.; Tang, Y.; Lu, H. Discovery of CD3+ CD19 +cells, a Novel Lymphocyte Subset with a Potential Role in Human Immunodeficiency Virus- Mycobacterium Tuberculosis Coinfection, Using Mass Cytometry. *Clin. Transl. Med.* **2021**, *11*, e681. [CrossRef] [PubMed]
75. Wang, J.; Wuethrich, A.; Sina, A.A.I.; Lane, R.E.; Lin, L.L.; Wang, Y.; Cebon, J.; Behren, A.; Trau, M. Tracking Extracellular Vesicle Phenotypic Changes Enables Treatment Monitoring in Melanoma. *Sci. Adv.* **2020**, *6*, eaax3223. [CrossRef]
76. Kadota, T.; Fujita, Y.; Yoshioka, Y.; Araya, J.; Kuwano, K.; Ochiya, T. Emerging Role of Extracellular Vesicles as a Senescence-Associated Secretory Phenotype: Insights into the Pathophysiology of Lung Diseases. *Mol. Asp. Med.* **2018**, *60*, 92–103. [CrossRef]

Disclaimer/Publisher's Note: The statements, opinions and data contained in all publications are solely those of the individual author(s) and contributor(s) and not of MDPI and/or the editor(s). MDPI and/or the editor(s) disclaim responsibility for any injury to people or property resulting from any ideas, methods, instructions or products referred to in the content.